Anomalous spectral lines and relic quantum nonequilibrium

Nicolas G. Underwood* and Antony Valentini†
Department of Physics and Astronomy,
Clemson University, Kinard Laboratory,
Clemson, SC 29634, USA
(Dated: January 4, 2017)

We describe general features that might be observed in the line spectra of relic cosmological particles should quantum nonequilibrium be preserved in their statistics. According to our arguments, these features would represent a significant departure from those of a conventional origin. Among other features, we find a possible spectral broadening (for incident photons) that is proportional to the energy resolution of the recording telescope (and so could be orders of magnitude larger than any intrinsic broadening). Notably, for a range of possible initial conditions we find the possibility of spectral line 'narrowing' whereby a telescope could observe a spectral line which is narrower than it should conventionally be able to resolve. We briefly discuss implications for the indirect search for dark matter.

arXiv:1609.04576v2 [quant-ph] 2 Jan 2017

I. INTRODUCTION

In the de Broglie-Bohm pilot-wave formulation of quantum theory [1–5], the Born probability rule has been shown to arise spontaneously through quantum 'relaxation' [6–13]–a dynamical process which is broadly similar to thermal relaxation in classical physics. The resulting relaxed or 'equilibrium' state obeys the Born rule so that, following relaxation, the theory becomes experimentally indistinguishable from conventional quantum theory. If one is to regard this relaxation–which occurs without the need for additional postulates–as the ultimate cause of conventional quantum probabilities, the question arises as to what preceded the relaxation. As such, pilot-wave theory allows for arbitrary ensemble probabilities [6–8, 14–22] and consequently may be regarded as a more general theory of which standard quantum theory is a special equilibrium case. A straightforward corollary to such a viewpoint is that 'quantum nonequilibrium'–defined generically as nonconformance to the Born rule–may have existed in the early universe, prior to relaxation [6, 7, 14, 15]. If so, then such primordial quantum nonequilibrium may have left traces that are still observable today, for example in the cosmic microwave background [17, 20, 23, 24].

Potentially it is also possible that quantum nonequilibrium may have survived in the statistical properties of some species of relic cosmological particles [8, 17, 18, 20, 25]. In a previous article [25] possible avenues through which nonequilibrium in particles could persist to this day were given and it was argued that detection of such relic nonequilibrium is in principle possible. This opens up the prospect that quantum nonequilibrium may play a role in contemporary experimentation–for example in the indirect search for dark matter. As yet however, it is unclear how this role would play out. The purpose of this article is to present a field theoretical account of the behaviour of quantum nonequilibrium under measurement that, whilst still far from an accurate description of the true workings of contemporary experiments (telescopes), takes at least a small step in this direction. Specifically, and for the reasons described below, we will take the example of telescopes tasked with the indirect detection of dark matter through spectral measurement of astrophysical photons, of which perhaps the best known is the Fermi-LAT [26]. We will draw comparisons to such telescopes throughout and section IV will be devoted to a discussion of the possible implications for the indirect search for dark matter. To structure our discussion, and to provide explicit calculations demonstrating our arguments, we present a model that we hope captures some of the general features that we might expect to observe should nonequilibrium indeed persist. On the one hand, the model–which is particularly simple and parameter free–performs the same ultimate function and shares some of the key characteristics of contemporary experiments that are potentially the most likely to observe relic nonequilibrium. On the other, we emphasise that the model is not a realistic representation of such experiments, and that the comparisons we will make are intended merely to provide context. Rather, our purpose is only to begin the discussion of the qualitative phenomena may ultimately be observed if relic nonequilibrium does indeed exist in the statistics of some particle species. The phenomena that we will discuss are something of a departure from those of a classical origin. For instance, if the model is taken at face value, any broadening of a spectral line will take place on a lengthscale corresponding to the energy resolution of the telescope used. In addition, lines may acquire double or triple bumps, or as we shall discuss, more exotic profiles. There also exists, for a variety of nonequilibrium distributions, the possibility of spectral line 'narrowing' in so much that a spectral line profile observed by a telescope would appear narrower than the energy resolution of the telescope could conventionally allow.

It has been argued [8, 17, 18, 20, 25] that quan-

* nunderw@clemson.edu
† antonyv@clemson.edu

tum nonequilibrium could in principle have survived for some species of relic cosmological particles. In speculating on such a possibility, two questions immediately arise. Firstly–what requisite properties must a particle species possess in order to have been created in a state of nonequilibrium, and in order to retain at least a portion of it to the present day? An answer to this question, and an identification of a viable candidate in current particle physics models would presumably allow one to assess the likelihood that relic nonequilibrium could be discovered. It has been argued [20, 25], for instance, that the decay of a nonequilibrium inflaton field may be a plausible mechanism for the production of such relics. A pilot-wave treatment of the inflaton field on the Bunch-Davies vacuum has been shown to exhibit trajectories that do not allow relaxation at all [17, 20]. Rather, any initial nonequilibrium in the inflaton field is simply scaled in proportion to physical wavelengths. In this respect, nonequilibrium from a pre-inflationary phase (if such a era existed) may have been conserved until (p)reheating, in which most of the matter in the universe is currently understood to have been created. Additionally, during inflation, field modes that are initially below the Planck scale are stretched to the scale at which current particle theories become meaningful. One could therefore conjecture that these so called trans-Planckian modes may have transferred exotic gravitational effects to conventional particle physics lengthscales [20, 25]. Of course, any discussion along these lines is highly speculative. An estimate of the likelihood of nonequilibrium surviving in particles to this day would depend delicately upon, not only the details of an assumed primordial cosmology, but also the particular particle physics model employed[1]. As these are two of the most uncertain areas of contemporary physics, in this article we will address a different question. For the purposes of this article, it will suffice to say that within whatever cosmological and particle physics theories ultimately stand the test of time, there may exist a reasonable window of opportunity for quantum nonequilibrium to survive to this day for some species of relic particle. We refer the reader to [25] for further discussion on this point.

The question we shall address is as follows. If quantum nonequilibrium did indeed exist in the statistics of a relic particle, then how might such nonequilibrium relics manifest themselves in present-day experiments? A basic requirement to avoid relaxation is that the particle must be only very minimally interacting. The particle would therefore almost certainly come under the heading dark matter, whether as the whole of the observed matter deficit or as part of a larger dark sector. Additionally, whilst it may be possible to synthesise a candidate species in a particle accelerator, the parent particles used would already have relaxed and so the products would necessarily display equilibrium statistics. We must therefore concern ourselves with astrophysical sources, which might conceivably contain particles that have not yet undergone complete relaxation [25]. In our discussion it will be useful to take, for the purposes of comparison and illustration, gamma-ray space telescopes concerned with the indirect detection of astrophysical candidates for dark matter generally referred to as weakly interacting massive particles (WIMPS). For example EGRET [27], Fermi-LAT [26], DAMPE [28], GAMMA-400 [29]. It is hoped that such experiments may observe photons from the annihilation or decay of WIMPs. If these WIMPs were themselves in a state of quantum nonequilibrium, then as argued in ref. [25] we might reasonably expect some of this nonequilibrium to remain in the statistics of the photons produced. Were such nonequilibrium photons to enter a telescope, then we might expect to see alterations to the spectrum observed, although the characteristics of these spectral alterations–the subject of this article–are not yet known.

By definition, dark matter does not interact directly with the electromagnetic field, and so the production of the photons that could be observed by these telescopes would happen at loop level, or through intermediary particle production. Despite the suppression that typically results from loop level interactions, it has long been argued [30–34] that the detection of photon emission from annihilating or decaying dark matter would provide excellent evidence for a dark matter candidate. Primarily this is because, in cold dark matter models, annihilation would produce two back-to-back photons of energy $E_\gamma = m_{\rm WIMP}$ and with only minimal intrinsic broadening (see for instance ref. [35]). Hence, observation of a spectral line would yield both the spatial location and the mass of the annihilating WIMP particles.

Of course, the telescopes are not perfectly precise in their measurements. A single reading of a photon of energy E_γ would satisfy what is termed the energy dispersion probability density function $D(E|E_\gamma)$, with a spread characterised by the energy dispersion $\Delta E/{E_\gamma}^2$. Many individual readings on an ensemble of photons with an actual spectrum $\rho_{\rm act}(E_\gamma)$ would produce an observed spectrum

$$\rho_{\rm obs}(E) = \int D(E|E_\gamma)\rho_{\rm act}(E_\gamma)dE_\gamma, \qquad (1)$$

that is convolved by the energy dispersion function $D(E|E_\gamma)$. In the context of spectral lines, it is pertinent to consider the relative width of the $D(E|E_\gamma)$ and $\rho_{\rm act}(E_\gamma)$ distributions. We may regard equation (1) in two separate regimes. Firstly, in the case of a higher resolution telescope where the width of $D(E|E_\gamma)$ is much smaller than any intrinsic spread in an actual

[1] Ref. [25] discusses an illustrative scenario for the gravitino ($\tilde{G}$), which arises in supergravity theories and is a proposed dark matter candidate.

[2] See for instance section 7 and figure 67 in [36].

line spectrum $\rho_{\rm act} = \rho_{\rm line}$, then we may approximate $D(E|E_\gamma) \to \delta(E-E_\gamma)$, and the observed spectrum would approximate the actual spectrum $\rho_{\rm obs}(E) \approx \rho_{\rm line}(E)$. In other words, a telescope of sufficient resolution may resolve the profile of the spectral line. Secondly, in the case of a lower resolution telescope, where the width of $D(E|E_\gamma)$ is much larger than the intrinsic spread in the actual line spectrum, we may approximate $\rho_{\rm act} = \rho_{\rm line}(E_\gamma) \to \delta(E_{\rm line} - E_\gamma)$ and the observed spectrum would instead approximate the energy dispersion function $\rho_{\rm obs}(E) \approx D(E|E_{\rm line})$. Hence, a telescope with an energy resolution that is inadequate to resolve the profile of an actual physical line, will instead observe a line whose profile is a function of the interaction between the telescope and the incident photon. In cold dark matter models of WIMPs, conventional line broadening occurs primarily due to the Doppler effect and is expected to produce an annihilation line with an intrinsic spread of 0.1% of $E_{\rm line}$ [35]. By comparison, the EGRET instrument aboard the Compton Gamma Ray Observatory that collected data from 1991-2000 achieved an energy dispersion of ∼20% [27]. The Large Area Telescope aboard the Fermi Gamma-ray Space telescope currently achieves around ∼10% [36]. The DAMPE telescope, which was launched in December 2015, achieves an energy dispersion of ∼1.5% [28]. The GAMMA-400 and HERD telescopes are proposed to be launched in the early 2020s and reach an energy resolution of ∼1% [29, 37]. All of these telescopes have energy dispersions that are appreciably larger than the expected 0.1% width of a WIMP annihilation line, and so could not be expected to resolve this conventional broadening. Instead, if a WIMP annihilation line were discovered, the observed line profile would closely approximate $D(E|E_{\rm line})$–a property of the telescope itself.

In contrast to the conventional broadening, and as we shall discuss, quantum nonequilibrium may be thought more properly to affect the interaction between the telescope and the photon, rather than the actual energy of the individual photons. The effect of quantum nonequilibrium is to alter the energy dispersion function $D(E|E_\gamma)$, rather than the actual spectrum $\rho_{\rm act}(E_\gamma)$. This is important as, naively, one might expect a higher resolution telescope (with smaller $\Delta E/E_\gamma$) to be preferential for detection of quantum nonequilibrium, but it appears that this may not be the case. Our analysis indicates that in the presence of quantum nonequilibrium, whilst higher resolution telescopes will remain more favourable for the discovery of a sharp spectral line, nonequilibrium signatures may be more apparent in spectra observed by lower resolution telescopes. Nonequilibrium will be most evident when the width of $D(E|E_\gamma)$, the energy dispersion $\Delta E/E_\gamma$, is larger than any intrinsic energy spread in $\rho_{\rm line}(E_\gamma)$–which we shall take as a working definition of lower resolution. Many of the current generation of telescopes are certainly within this regime. As such, if one were to accept these arguments and those we shall develop through the model below, then for many of the current generation of telescopes nonequilibrium line effects could in principle dominate conventional line broadening.

Our paper is organised as follows. In section II we present an idealised and parameter-free field-theoretical model of a spectral measurement of the electromagnetic field. This will be sufficiently simple as to permit an explicit solution to the (functional) Schrödinger equation. In section III we present the pilot-wave description of the model, we discuss how nonequilibrium may affect spectral lines, and we provide some explicit calculations. In section IV we comment on the limitations of the model and discuss possible implications for the indirect search for dark matter.

II. MODEL OF IDEAL ELECTROMAGNETIC ENERGY MEASUREMENT AND QUANTUM FIELD-THEORETICAL SPECTRAL RECONSTRUCTION

The γ-ray sky is extremely faint. So faint in fact, that γ-photons generally arrive one by one into the telescopes that are designed to detect them. These telescopes are therefore designed to measure the total energy of each individual γ-photon as it arrives, and as such bear a greater resemblance to particle physics experiments than to conventional telescopes. When a photon enters the telescope a triggering mechanism is activated (see for instance refs. [36, 38]). The telescope will then record, amongst other data (and perhaps after some processing), a single value for the energy of the photon. For an incident photon of true energy E_γ, the possible recorded energy values E will satisfy a probability distribution $D(E|E_\gamma)$. The spread of this distribution is most simply quantified by the so-called energy dispersion $\Delta E/E_\gamma$–roughly speaking the standard deviation of the distribution around E_γ, stated in proportion to E_γ. As a first approximation to the behaviour of such telescopes, we could consider an idealised von Neumann measurement of the total energy of the electromagnetic field. We could assume that in any individual energy measurement (or event) there is exactly one photon present. The observed spectrum will then be composed of the measured energies of many individual photons. To avoid complications associated with the localisability of photons, we shall take the electromagnetic field to be quantised within a region that corresponds to the dimensions of the telescope. In each measurement, exactly one photon is assumed to exist within this region. As we shall discuss below, an analogue energy dispersion will naturally arise in such a model.

We may base such a model on the de Broglie-Bohm pilot-wave description of standard von Neumann measurements [4]. For the case of the measurement of an observable $\mathcal{A}$ with a discrete and non-degenerate spectrum, a system with wave function $\psi(q)$ is coupled to a pointer with wave function $\phi(y)$ via an interaction Hamiltonian

$$H_{\rm I} = g\mathcal{A}p_y, \tag{2}$$

where p_y is the conjugate momentum operator of the pointer. The coupling constant g is taken to be zero prior to the measurement which begins at $t = 0$. Thereafter g is taken to be large enough to ensure that the subsequent evolution is dominated by the interaction Hamiltonian. With this stipulation, the Schrödinger equation takes the simple form

$$\partial_t \Psi = -g\mathcal{A}\partial_y \Psi. \tag{3}$$

Then, since we have assumed the spectrum of $\mathcal{A}$ to be discrete and non-degenerate, we may decompose the system wave function as $\psi(q) = \sum_n c_n \psi_n(q)$, with $\psi_n(q)$ and a_n denoting the respective eigenstates and corresponding eigenvalues of $\mathcal{A}$. The system evolves as

$$\psi(q)\phi(y) \to \sum_n c_n \psi_n(q)\phi(y - g a_n t) \tag{4}$$

and the outcome probability of the experiment is determined by the effective distribution of the pointer y–the marginal Born distribution (hereby called the measured distribution), $\rho_{\text{meas}}(y) := \int |\Psi(q, y)|^2 dq$. Initially the different components of the summation (4) overlap in the configuration space, producing interference in the measured distribution. Over the course of the measurement however, the different components travel within the configuration space in the direction of increasing pointer coordinate y. Each component travels at a speed proportional to its eigenvalue a_n. Consequently, if we prepare the pointer in some reasonably compact state (perhaps a Gaussian as we shall do later), then after some sufficient time (deemed the duration of the measurement), the different components of the summation will have separated. The measured distribution produced,

$$\rho_{\text{meas}}(y) = \sum_n |c_n|^2 |\phi(y - g a_n t)|^2, \tag{5}$$

no longer exhibits interference and will display disjoint regions of support. An experimenter familiar with their apparatus will know about these disjoint regions within which they may find the pointer once the measurement has concluded. They will also understand that each one of these regions corresponds to a particular eigenvalue of the operator $\mathcal{A}$. The conclusion of one such measurement is to find the pointer in the nth region corresponding to the nth eigenvalue, with a probability of $|c_n|^2$. The discrete spectrum, $|c_n|^2$, may then be reconstructed by repeated measurements over an ensemble[3]. In the standard formulation of quantum mechanics, wave function collapse occurs at the end of each measurement in order to ensure that the pointer is found in a single one of the disjoint regions. In the de Broglie-Bohm account, the system (which always occupies a definite position in the configuration space) is simply found in one of the regions, with no need for any non-unitary evolution. Instead an 'effective collapse' occurs as, once the components of the wave function (4) have properly separated, subsequent evolution of the system configuration is determined solely by the component that contains the configuration. The spatial separation of the other components is enough to ensure that they become irrelevant to the future evolution of the configuration and hence may be disregarded in future calculations.

The formulation as presented so far only accounts for the measurement of observables with discrete spectra. We cannot however associate disjoint regions in y to eigenvalues on a continuous (energy) scale. Instead, given a particular pointer position we must make an estimate of the energy of the incident photon. In doing so we will find an energy dispersion behaviour similar to that found in experiment. In our model telescope we measure the total (normal-ordered) Hamiltonian of the free-space electromagnetic field, $:H_{\text{EM}}:$, so that

$$H_{\text{I}} = g{:}H_{\text{EM}}{:}p_y. \tag{6}$$

For an initial single photon state $|E_\gamma\rangle$ we have the simple evolution

$$|E_\gamma\rangle\,|\phi(y)\rangle \to |E_\gamma\rangle\,|\phi(y - gE_\gamma t)\rangle\,. \tag{7}$$

Although the photon has an exact energy, the quantum uncertainty in the initial position of the pointer will produce some uncertainty in the pointer position at any later time. The probability density of finding the pointer at a position y is given by

$$\rho_{\text{meas}}(y, t) = |\phi(y - gE_\gamma t)|^2. \tag{8}$$

With many such pointer positions (so that we knew $\rho_{\text{meas}}(y, t)$ perfectly) we could infer an E_γ. In a single measurement however, we will find the pointer at a single definite position and, as is the case with experiment, we will assign a single energy to each incident photon. In the case where there is finite pointer uncertainty there is no way infer the photon energy E_γ perfectly from the position of the pointer. The best we can do is to assign the photon energy that was most likely to have caused that particular pointer position. Supposing the pointer packet to be Gaussian, as we shall do henceforth, this amounts to assigning

$$E = y/gt. \tag{9}$$

We shall take the initial pointer packet $|\phi(y)|^2$ to be centred on $y = 0$ and of variance σ_y^2. With this stipulation the energy dispersion function becomes

$$D(E|E_\gamma) = \frac{1}{\sqrt{2\pi}} \frac{gt}{\sigma_y} e^{-\frac{1}{2}\left(\frac{gt}{\sigma_y}\right)^2 (E - E_\gamma)^2}. \tag{10}$$

[3] In reference [25] it was shown that the existence of quantum nonequilibrium in the measured system will tend to distort the outcome of such measurements on systems with discrete spectra.

Since this is a Gaussian, the energy dispersion (defined as the fractional minimum 68% containment window) is simply the fractional standard deviation,

$$\frac{\Delta E}{E_\gamma} = \frac{\sigma_y}{gtE_\gamma}. \tag{11}$$

In order to determine to what extent a set of data (a list of individual energies) is consistent with some hypothetical spectrum, it will be useful to know what distribution $\rho_{\rm obs}(E)$ we expect to observe in our data given some actual spectrum $\rho_{\rm act}(E_\gamma)$. This is given by the convolution (1) as

$$\rho_{\rm obs}(E) = \int_0^\infty \rho_{\rm act}(E_\gamma)\frac{1}{\sqrt{2\pi}}\frac{gt}{\sigma_y}e^{-\frac{1}{2}\left(\frac{gt}{\sigma_y}\right)^2(E-E_\gamma)^2}\,dE_\gamma, \tag{12}$$

which in this case is a simple 'Gaussian blur' (or Weierstrass transform) of the actual spectrum.

The duration t of the measurement appears in the denominator of equation (11), perhaps giving the appearance that the precision improves with the run time of the measurement. In a sense this is true, but the formulation so far has only featured time as a factor in the quantity gt. A more impulsive coupling constant (that is to say that g is larger for the duration of measurement) would improve the precision in an analogous manner. In addition to this, in section III it will be useful to rescale the pointer variable y in terms of its initial standard deviation σ_y. In doing so, it will turn out that σ_y only appears in the quantity gt/σ_y. Consequently, a narrower pointer packet would also produce an analogous improvement in precision. With this in mind, we may rephrase the model in terms of the precision of the experiment (the energy dispersion $\Delta E/E_\gamma$). We define the rescaled time variable,

$$T = \frac{gtE_\gamma}{\sigma_y} = \left(\frac{\Delta E}{E_\gamma}\right)^{-1}, \tag{13}$$

which is effectively the resolution of the telescope

The variables g, σ_y and t are the only free parameters in this model thus far. The definition (13) allows us to absorb these into the single easily interpreted quantity, T, leaving our model effectively parameter-free. The true energy E_γ is included in this definition so that the rescaled time (13) is exactly the reciprocal of the energy dispersion (11)–no matter the true energy of the incident photon. Thus, for instance, our (ideal) model may reproduce a roughly EGRET dispersion of 20% at $T = 5$, a roughly Fermi-LAT dispersion of 10% at $T = 10$ or a roughly GAMMA-400/HERD dispersion of 1% at $T = 100$.

III. NONEQUILIBRIUM SPECTRAL LINES

An experimenter performing a search for spectral lines with the methodology developed in section II will record their data according to equation (9) and expect this data to be distributed according to equation (12), whether or not a spectral line is present. If in addition to a background an annihilation line is indeed present, then the actual spectrum may be decomposed as

$$\rho_{\rm act}(E_\gamma) = \left(n_{\rm bkg}\rho_{\rm act}^{\rm bkg}(E_\gamma) + n_{\rm sig}\delta(E\gamma - E_{\rm line})\right)/n_{\rm tot}, \tag{14}$$

where $n_{\rm bkg}$ and $n_{\rm sig}$ are the respective numbers of background and signal photons. The total number of photons recorded is denoted $n_{\rm tot}$. As discussed in section I, the representation of a line as a delta function is appropriate when the telescope is not capable of resolving any intrinsic spread caused by conventional broadening. Furthermore, it is well known that de Broglie-Bohm pilot-wave theory does not allow for back reaction–in the sense that the particular configuration of an individual system does not affect the evolution of the quantum state. This means that, as the energy eigenvalue of the photon is a property of the quantum state of the EM field rather than of its particular configuration, the delta distribution of the signal in equation (14) is correct even in the case of quantum nonequilibrium. Put differently, conventional physical effects alter the profile of spectral lines by altering the energy eigenvalues of the individual photons. Quantum nonequilibrium, on the other hand, affects the ensemble distribution of field amplitudes while having no effect on the eigenvalues appearing in the quantum state itself.

That said, any quantum nonequilibrium present in the annihilation photons will affect the observed spectrum by altering the statistics of the interaction of the line photons with the telescope. The energy dispersion $D(E|E_{\rm line})$ is the spectrum observed given a source of monochromatic photons of energy $E_{\rm line}$. We would expect deviations from this in the presence of nonequilibrium. We therefore regard the effect of quantum nonequilibrium to be to alter the function $D(E|E_\gamma)$ rather than to alter the actual spectrum of the incident photons (in contrast with conventional effects). We shall denote the new energy dispersion function $D_{\rm noneq}(E|E_\gamma)$. Its properties are the main focus of this work. Under the measurement of an equilibrium background with a nonequilibrium line signal, then, we would expect to observe a spectrum with the background convolved by $D(E|E_\gamma)$ in the standard manner (1) and with a nonequilibrium signal distribution superimposed,

$$\begin{aligned}\rho_{\rm obs}(E) = &\int_0^\infty \frac{n_{\rm bkg}}{n_{\rm tot}}\rho_{\rm act}^{\rm bkg}(E_\gamma)D(E|E\gamma)\mathrm{d}E_\gamma \\ &+ \frac{n_{\rm sig}}{n_{\rm tot}}D_{\rm noneq}(E|E_{\rm line}).\end{aligned} \tag{15}$$

Generally speaking, we may divide the characteristic properties of nonequilibrium spectral lines $D_{\rm noneq}(E|E_\gamma)$ into two categories.

The first property of the function $D_{\rm noneq}(E|E_\gamma)$ concerns its typical lengthscale. As is perhaps unsurprising,

it will turn out that $D_{\rm noneq}(E|E_\gamma)$ has a width of order $\Delta E/E_\gamma$, the width of the equilibrium function $D(E|E_\gamma)$. As this width defines the energy resolution of the telescope, we may expect telescopes of differing energy resolution to observe differing amounts of spectral broadening. The amount of broadening will be proportional to the resolution of the telescope. As we shall see, the constant of proportionality here may be smaller than unity, and hence there is the possibility of spectral narrowing in the sense that the width of $D_{\rm noneq}(E|E_\gamma)$ may be smaller than the width of $D(E|E_\gamma)$. As our time variable has been defined as $T = (\Delta E/E_\gamma)^{-1}$, the typical lengthscale of the function $D_{\rm noneq}(E|E_\gamma)$ will shorten as the system evolves and as time increases the model in effect describes the outcome of increasingly higher resolution telescopes. Later, it will be convenient to measure deviations from a perfect measurement in units of this typical lengthscale, so that we may in effect remove the narrowing of $D_{\rm noneq}(E|E_\gamma)$.

The second category of properties of the function $D_{\rm noneq}(E|E_\gamma)$ concerns its profile and its possible fine grained structure. Upon evolving with T, a nonequilibrium distribution will undergo a dynamical relaxation. This process will in most cases lead to the formation of bumps, tails and large spikes in $D_{\rm noneq}(E|E_\gamma)$–features that will evolve into finer structure and eventually become too fine to resolve. A particular telescope (of a given resolution) is represented by a snapshot in this evolution. Thus, any single one of these phenomena could be observed by a telescope of appropriate resolution. The most dramatic departures from $D(E|E_\gamma)$ will tend to occur for lower resolution telescopes where the incoming nonequilibrium may not have been significantly disturbed. In these cases, there has been less opportunity for relaxation. This is however not to say that the model indicates that lower resolution telescopes are altogether preferable for a discovery of nonequilibrium. As we shall discuss, there are some features of higher resolution measurements that may prove beneficial.

A. De Broglie-Bohm description of measurement

To study quantum nonequilibrium, we first need a de Broglie-Bohm description of the measurement. To develop such a de Broglie-Bohm description, we first need a coordinate representation of the electromagnetic field. We will work in the Coulomb gauge, $\nabla.\mathbf{A}(\mathbf{x},t) = 0$, with the field expansion

$$\mathbf{A}(\mathbf{x},t) = \sum_{\mathbf{k}s} \left[A_{\mathbf{k}s}(t)\mathbf{u}_{\mathbf{k}s}(\mathbf{x}) + A^*_{\mathbf{k}s}(t)\mathbf{u}^*_{\mathbf{k}s}(\mathbf{x}) \right], \qquad (16)$$

where the functions

$$\mathbf{u}_{\mathbf{k}s}(\mathbf{x}) = \frac{\boldsymbol{\varepsilon}_{\mathbf{k}s}}{\sqrt{2\varepsilon_0 V}} e^{i\mathbf{k}.\mathbf{x}} \qquad (17)$$

and their complex conjugates define a basis for the function space and V is a normalisation volume. To avoid duplication of basis elements $\mathbf{u}^*_{\mathbf{k}s}$ with $\mathbf{u}_{-\mathbf{k}s}$, the summation (16) should be understood to extend over only half the possible wave vectors $\mathbf{k}$. See for instance reference [39]. This expansion allows one to write the energy of the electromagnetic field as

$$U = \frac{1}{2}\int_V \mathrm{d}^3x \left(\varepsilon_0 \mathbf{E}^2 + \frac{1}{\mu_0}\mathbf{B}^2 \right) \qquad (18)$$

$$= \sum_{\mathbf{k}s} \frac{1}{2} \left(\dot{A}_{\mathbf{k}s}\dot{A}^*_{\mathbf{k}s} + \omega^2_{\mathbf{k}} A_{\mathbf{k}s}A^*_{\mathbf{k}s} \right), \qquad (19)$$

where $\omega_{\mathbf{k}} = c|\mathbf{k}|$. Equation (19) corresponds to a decoupled set of complex harmonic oscillators of unit mass. We prefer instead to work with real variables and so we decompose $A_{\mathbf{k}s}$ into its real and imaginary parts

$$A_{\mathbf{k}s} = q_{\mathbf{k}s1} + iq_{\mathbf{k}s2}. \qquad (20)$$

One may then write the free field Hamiltonian as

$$H_0 = \sum_{\mathbf{k}sr} H_{\mathbf{k}sr} \qquad (21)$$

with $r = 1, 2$, where

$$H_{\mathbf{k}sr} = \frac{1}{2}\left(p^2_{\mathbf{k}sr} + \omega^2_{\mathbf{k}} q^2_{\mathbf{k}sr} \right), \qquad (22)$$

and where $p_{\mathbf{k}sr}$ is the momentum conjugate of $q_{\mathbf{k}sr}$. The variables y and $\{q_{\mathbf{k}sr}\}$ are the configuration-space 'beables'. Together they specify the configuration of the field-pointer system. By rescaling the beable coordinates,

$$Q_{\mathbf{k}sr} = \sqrt{\frac{\omega_{\mathbf{k}}}{\hbar}} q_{\mathbf{k}sr}, \quad Y = \frac{y}{\sigma_y}, \qquad (23)$$

we may write the Schrödinger equation as[4]

$$\partial_T \psi + \frac{1}{2}\sum_{\mathbf{k}sr} \frac{E_{\mathbf{k}}}{E_\gamma} \left(-\partial^2_{Q_{\mathbf{k}sr}} + Q^2_{\mathbf{k}sr} - 1 \right) \partial_Y \psi = 0. \qquad (24)$$

By using a method similar to that used in [25] (based on general expressions derived in [40]), one may arrive at guidance equations for a general field-pointer state,

$$\partial_T Q_{\mathbf{k}sr} = \frac{E_{\mathbf{k}}}{E_\gamma} \left(-\frac{1}{3}\psi\partial_{Q_{\mathbf{k}sr}}\partial_Y\psi^* + \frac{1}{6}\partial_Y\psi\partial_{Q_{\mathbf{k}sr}}\psi^* + \frac{1}{6}\partial_{Q_{\mathbf{k}sr}}\psi\partial_Y\psi^* - \frac{1}{3}\psi^*\partial^2_{Q_{\mathbf{k}sr}}\psi \right) / |\psi|^2, \qquad (25)$$

$$\partial_T Y = \sum_{\mathbf{k}sr} \frac{E_{\mathbf{k}}}{E_\gamma} \left(-\frac{1}{6}\psi\partial^2_{Q_{\mathbf{k}sr}}\psi^* + \frac{1}{6}\partial_{Q_{\mathbf{k}sr}}\psi\partial_{Q_{\mathbf{k}sr}}\psi^* - \frac{1}{6}\psi^*\partial^2_{Q_{\mathbf{k}sr}}\psi + \frac{1}{2}\left(Q^2_{\mathbf{k}sr} - 1 \right)|\psi|^2 \right) / |\psi|^2. \qquad (26)$$

[4] In equations (24), (25), and (26), E_γ should be understood to be a reference energy that will later refer to the energy of the incident photon.

These are the de Broglie-Bohm equations of motion for the configuration of the field-pointer system.

We will assume that, prior to the spectral measurement, a single mode of the field 'contains' a nonequilibrium photon of energy E_γ, whilst all others are in their equilibrium vacuum states. We shall refer to the beable associated with this mode simply as Q. Henceforth, all summations or products over $\mathbf{k}sr$ should be understood to exclude the mode that contains the photon. With this in mind, the wave function(al) of the pointer-field system may be written

$$\psi = \underbrace{(2\pi)^{-\frac{1}{4}} \exp\left[-\frac{1}{4}(Y-T)^2\right]}_{\phi} \times \underbrace{2^{\frac{1}{2}}\pi^{-\frac{1}{4}} Q \exp\left[-\frac{1}{2}Q^2\right]}_{\chi_1} \prod_{\mathbf{k}sr} \underbrace{\pi^{-\frac{1}{4}} \exp\left[-\frac{1}{2}Q_{\mathbf{k}sr}^2\right]}_{\chi_0}. \tag{27}$$

Here, χ_0 and χ_1 refer to harmonic oscillator ground and first excited states respectively. With this specific state, the general guidance equations (25) and (26) become

$$\begin{aligned} \partial_T Q &= \frac{1}{6}\left(\frac{1}{Q} - Q\right)(Y-T), \\ \partial_T Q_{\mathbf{k}sr} &= -\frac{1}{6}\frac{E_{\mathbf{k}}}{E_\gamma} Q_{\mathbf{k}sr}(Y-T), \\ \partial_T Y &= \frac{1}{6Q^2} + \frac{1}{3}Q^2 + \frac{1}{6} + \sum_{\mathbf{k}sr} \frac{E_{\mathbf{k}}}{E_\gamma}\left(\frac{1}{3}Q_{\mathbf{k}sr}^2 - \frac{1}{6}\right). \end{aligned} \tag{28}$$

We have coupled the pointer to the total energy of the field. This total energy is simply a sum of the energies of each mode, all but one of which are normal ordered vacuum modes–and hence of zero energy. Quantum mechanically then, the vacuum modes are effectively uncoupled from the pointer. This is evident from the simple Schrödinger evolution (27). One might expect the same to hold for the de Broglie-Bohm treatment, however it appears that this is not the case. The guidance equations (28) describe a system in which the beable of each vacuum mode, $Q_{\mathbf{k}sr}$, is coupled directly to the pointer, and through their interaction with the pointer they are coupled indirectly to each other. (For more details on the energy measurement of a vacuum mode see [25].) Accordingly, this is a rather complex system, and before returning to it at the end of this section we will treat what may be considered a first approximation.

B. Reduced two dimensional model

As a first approximation to the full de Broglie-Bohm model of equations (28), we consider a system in which the pointer beable is decoupled from the vacuum mode beables (just as, in the standard quantum description, the vacuum modes are decoupled from the pointer). In this reduced system, only the beable Q of the excited mode will affect the evolution of the pointer, and so we may treat our system as effectively two dimensional.

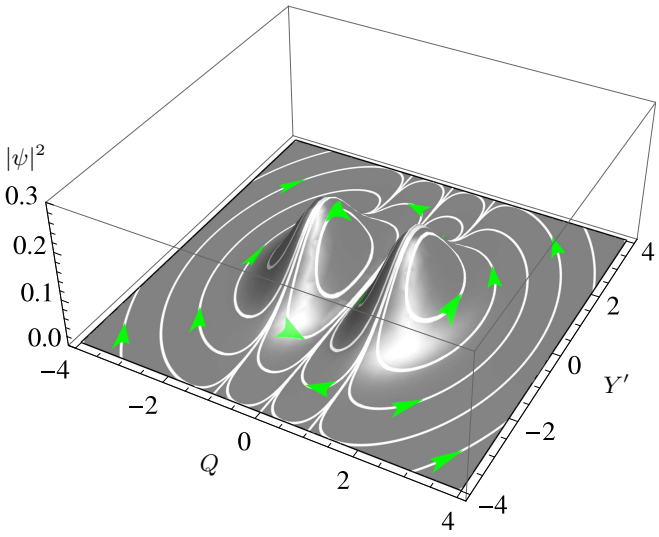

FIG. 1. Periodic orbits produced by the guidance equations (33) contrasted with the quantum equilibrium distribution (30). The pointer coordinate Y' may be thought of as measuring the deviation from a perfect energy reading in units of the energy dispersion, $Y' = (E - E_\gamma)/\Delta E$.

Rather than translating pointer positions directly into energy readings, as in equation (9), it is convenient to use the variable

$$Y' = Y - T. \tag{29}$$

This has some useful properties. Firstly, in a configuration space measured by the coordinates (Q, Y') the evolution of the quantum equilibrium distribution is frozen,

$$|\psi|^2 = \frac{1}{\sqrt{2\pi}} \exp\left(-\frac{1}{2}Y'^2\right) \frac{2}{\sqrt{\pi}} Q^2 \exp\left(-Q^2\right). \tag{30}$$

We have effectively shifted to the 'frame' of quantum equilibrium. Secondly, for any particular system configuration (Q, Y') the energy that would be recorded by the telescope is given by

$$\begin{aligned} E &= E_\gamma\left(1 + \frac{Y'}{T}\right) \\ &= E_\gamma + Y'\Delta E, \end{aligned} \tag{31}$$

or equivalently

$$Y' = (E - E_\gamma)/\Delta E. \tag{32}$$

Thus a pointer position of $Y' = 0$ will constitute a perfect reading of the energy E_γ, and any deviations from this will be measured in units of the energy resolution $\Delta E/E_\gamma = 1/T$. In this regard, we may use the variable

Y' to explore the shape of the nonequilibrium spectral line with respect to the expected line width.

In terms of these coordinates the guidance equations

$$\begin{aligned}\partial_T Q =& \frac{1}{6} Y' \left(\frac{1}{Q} - Q \right), \\ \partial_T Y' =& \frac{1}{6Q^2} + \frac{1}{3} Q^2 - \frac{5}{6}\end{aligned} \tag{33}$$

are also time-independent. They are found to yield simple periodic orbits (see figure 1) about four stationary points at $(\pm\sqrt{5 \pm \sqrt{17}}/2, 0)$. The orbits do not cross boundaries in the configuration space at $Q = 0$ and $Q = \pm 1$, corresponding to stationary points of $|\chi_1|^2$.

The paths taken by the trajectories may be solved for by finding a function of configuration space, $G(Q, Y')$, that is conserved along trajectories. The paths will then be the contour lines of such a function. Along the trajectory, the rate of change of G is given by its material derivative, $v.\nabla G$. We may solve $v.\nabla G = 0$ by separation of variables, and for a particular choice of integration constants, may arrive at the parameter free form

$$G = Y'^2/2 + Q^2 - \ln|Q| - \ln|Q^2 - 1|. \tag{34}$$

By construction G is conserved along trajectories. This is similar to the equation for a circle, except for the logarithm terms that diverge at $Q = \pm 1$ and $Q = 0$, preventing trajectories crossing these boundaries. These orbits are contrasted with quantum equilibrium in figure 1. An initial distribution restricted to a region of configuration space in which G is bounded above by some value $G_{\max}$ will evolve into a distribution which is restricted to the same region. The resulting marginal pointer distribution will be confined to a region centred on $Y' = 0$ and of definite half-width

$$Y'_{\max} = \begin{cases} 2\sqrt{2(G_{\max} - 1.62105)} & \text{if} \quad |Q| > 1 \\ 2\sqrt{2(G_{\max} - 1.22552)} & \text{if} \quad |Q| < 1 \end{cases}. \tag{35}$$

Since $Y'_{\max}$ is constant and equal to the maximum value of $(E - E_\gamma)/\Delta E$, we may conclude that the amount of any spectral line broadening or narrowing will be proportional to ΔE and hence to the resolution of the telescope. For instance, figure 1 shows that a distribution initially clustered around the four stationary points $(\pm\sqrt{5 \pm \sqrt{17}}/2, 0)$ will remain so. Such a distribution could produce a spectral line that is, say, twice as narrow as an equilibrium line. Since this ratio is conserved in time and $T = (\Delta E/E_\gamma)^{-1}$, the line will be twice as narrow regardless of the resolution of the telescope or of the energy of the line. In general, however, we expect to see a dynamic relaxation that will contribute transients.

It has been well documented [6–13] that quantum nonequilibrium distributions tend to relax towards quantum equilibrium (as long as, in analogy with classical systems, there is no conspiracy in the initial conditions). This happens in a manner that is broadly analogous to thermal relaxation in classical mechanics. To illustrate, suppose for instance that a classical system had a distribution ρ that was initially confined to some phase-space region and with some initially constant probability density $\rho = \rho_0$. As phase space volumes and probability densities each satisfy the Liouville property (they are conserved along trajectories), ρ will remain confined to a region of the same volume and with the same $\rho = \rho_0$ thereafter. Consequently, the exact Gibbs entropy $S = -k \int \mathrm{d}\Omega \rho \ln \rho$ (whose integrand is zero in the region in which $\rho = 0$ and constant in the region in which $\rho = \rho_0$) will be preserved. Over time, however, the region in which ρ is non-zero will tend to become stretched and warped until such a time when it will display a great deal of fine-grained structure. Any subsequent experimental blurring or coarse graining will obscure this fine structure, making the distribution appear to have been spread out over a larger phase space volume. On a coarse-grained level entropy will have risen. The inability to resolve the fine structure (eventually) results directly in an increase in the standard experimental notion of entropy. Of course, fine structure would be difficult to reproduce were one attempting to reconstruct ρ from a finite number of measurements on an ensemble. (A finite number of measurements produces an increase in entropy that is analogous, if not the same, as the coarse graining that is commonly held to be the direct cause of entropy rise.) A similar process occurs in pilot-wave dynamics, where the ratio $\rho/|\psi|^2$ is conserved along trajectories (in configuration space). The distribution ρ develops a fine-grained structure, in such a way that on a coarse-grained level it becomes indistinguishable from $|\psi|^2$. A co-moving configuration space volume may shrink if moving to a region of larger $|\psi|^2$. Correspondingly, the state of maximum entropy is given by $\rho = |\psi|^2$, rather than a uniform distribution as it is Hamiltonian mechanics. Nevertheless, we observe the same stretching and warping that is characteristic of classical thermodynamic relaxation. In our field-pointer system, trajectories with larger orbits have larger periods. Any two systems that are initially close in the configuration space eventually become 'out of phase', producing 'swirling' patterns that eventually become too fine to resolve. Any coarse graining–for example in binning the energy readings–will smooth over the fine structure. However the simple trajectories produced by equations (33) do not result in full relaxation to $|\psi|^2$. Instead, a stationary distribution is reached that is characteristic of the initial nonequilibrium.

Quantum nonequilibrium is defined as a deviation from the Born rule, and as such could take many different forms. The nature of the quantum nonequilibrium that could be present in the photon statistics–the shape, and extent of the deviations–remains an open question. In order to provide some explicit examples, we shall use a simple parameterisation of the relative width of nonequilibrium to equilibrium. We introduce a widening parameter w to produce (normalised) nonequilibrium distributions

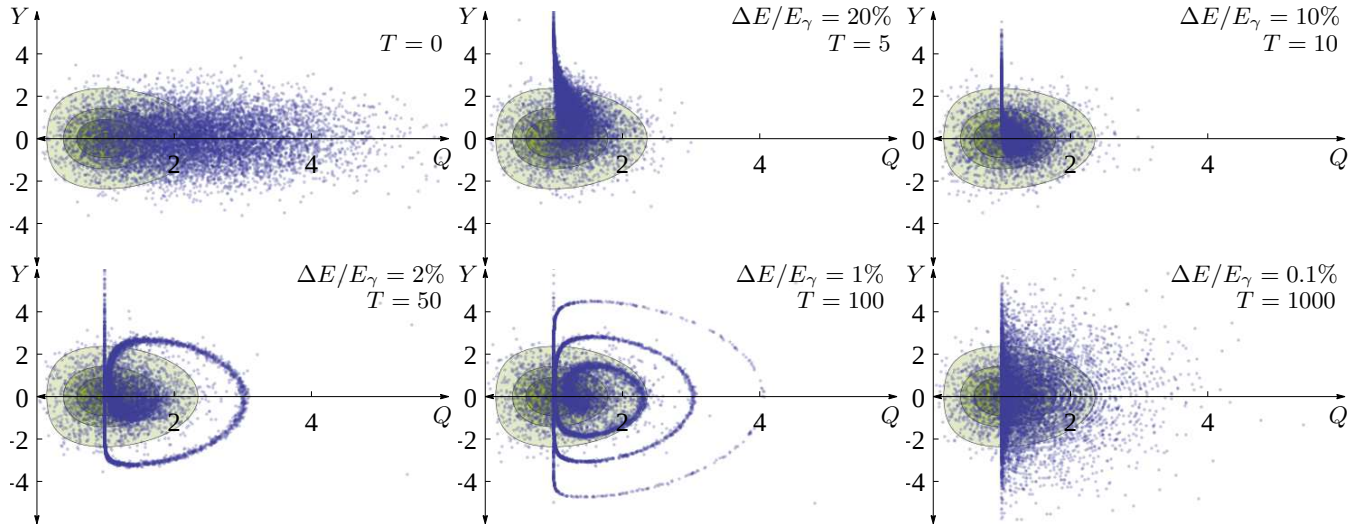

FIG. 2. The evolution of a nonequilibrium ensemble of spectral measurements (represented by 10,000 points). The top-left frame displays the initial nonequilibrium state which has been chosen to be twice as wide ($w = 2$) as the equilibrium distribution (displayed in green for comparison). Subsequent frames may be thought of as corresponding to subsequent times in the evolution, or since $\Delta E/E_\gamma = T^{-1}$ they may equally be thought of as corresponding to individual measurements at the stated resolution. The variable Q is associated with the field mode that 'contains' the photon. Only $Q > 0$ is shown as the behaviour is identical for $Q < 0$. The variable $Y = (E - E_\gamma)/\Delta E$ denotes the accuracy of the reading in units of the energy dispersion of the model telescope. Distributions that are initially sufficiently wider than equilibrium will tend to be confined to the regions $|Q| > 1$ (cf. figure 1). For lower resolution telescopes (frames 2 and 3) the energy of the effective line will tend to be overestimated and the line will be broadened. For mid-resolution telescopes, swirls begin to form that present themselves as bumps or shelves in the profile of the spectral line. The final frame shows a relatively high resolution telescope for which the structure in the nonequilibrium distribution has become very fine. This represents the maximum extent of relaxation that is available to the system. Ideal model telescopes that are of high enough resolution to exist within this regime would observe the same spectral profile (albeit in units of their own ΔE). The spectral lines for produced by another widened distribution ($w = 4$) are shown in figure 3.

from (30) as

$$\rho_0(Q, Y') = |\psi_0(Q/w, Y')|^2/w. \tag{36}$$

The evolution of an initial double width ($w = 2$) distribution is shown in figure 2. (In this figure (and also in figure 4) we show only the region $Q > 0$ of the configuration space, since the behaviour is identical for $Q < 0$.) Initial nonequilibrium distributions that are wider than equilibrium will tend to have more of their support confined to the $|Q| > 1$ regions of the velocity field (cf. figure 1). Hence, their early evolution will tend to produce spectral lines that overstate the true energy and exhibit spectral broadening. As the configuration space swirls start forming, the spectral line will display bumps or shelves. Eventually, enough of these will have formed that their presence will not be seen in the marginal distribution (on a coarse-grained level). The spectral line will appear widened, though centred on the true energy. These line features are shown in figure 3 for an initial $w = 4$ nonequilibrium state.

Initial nonequilibrium distributions that are narrower than equilibrium will tend to have more of their support confined to the region $|Q| < 1$. In this region the trajectories are approximately circular (unless they are initially very close to $Q = 0$ or $Q = \pm 1$). For large times, or equivalently for a relatively high resolution model telescope, the spectral line produced may be very similar to that produced in equilibrium. For lower resolution telescopes, the relaxation generally produces spectral lines that are narrower than the equilibrium line. As the system evolves, the narrowed line splits into two sharp lines and then three. These remain within the support of the equilibrium line. Increasing numbers of lines are produced that are distributed in a manner that exhibits an increasingly Gaussian profile. The evolution of a $w = 1/4$ initial nonequilibrium state is shown in figure 4 and the corresponding spectral lines are shown in figure 5.

To summarise, the characteristic modifications of the spectral lines produced by our model may be divided into two categories.

In the first category, the effect of quantum nonequilibrium is to change the statistics of the interaction between the telescope and the signal photons rather than the energy of the signal photons. The standard line spectrum $D(E|E_\gamma)$ is changed to $D_{\text{noneq}}(E|E_\gamma)$. These effects have a typical lengthscale of order $\Delta E/E_\gamma$, the resolution of the telescope. Thus, different telescopes (with differing resolution $\Delta E/E_\gamma$) will observe different effects. For higher resolution telescopes, the effects could be small compared to conventional broadening and so may go unnoticed. Conversely, for a telescope that is not capable

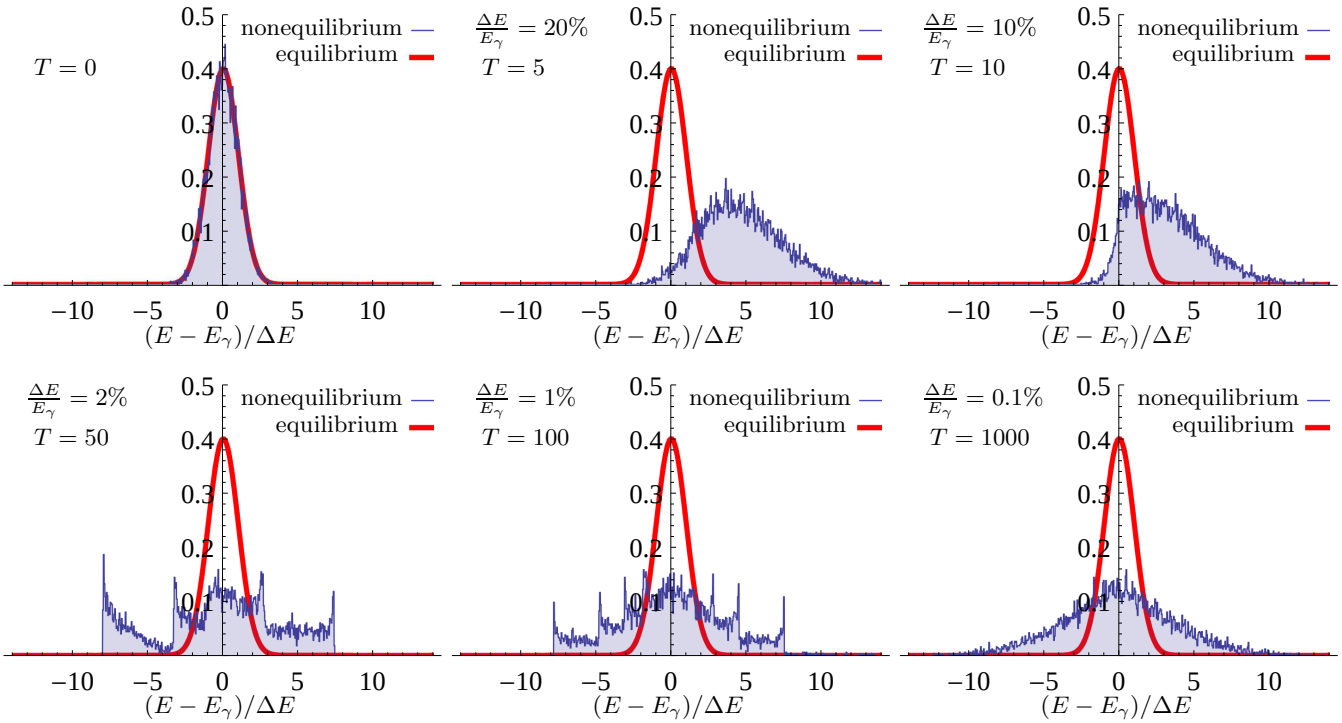

FIG. 3. Spectral line profiles produced by an initial $w = 4$ quantum nonequilibrium, contrasted with the equilibrium line (the standard energy dispersion function). Each frame corresponds to a model telescope with different resolution. (For instance, the third frame shows a line produced by a model telescope with a roughly Fermi-LAT resolution of $\Delta E/E_\gamma = 10\%$.) The lines are given by the marginal distributions of the frames in figure 2, except that in this case we have taken $w = 4$ to help illustrate the behaviour more clearly. The energies that are recorded are measured in units of the energy dispersion of the frame. (For example, in absolute energy units and for a given value of E_γ, the equilibrium spectral line in frame 3 is 100 times the width of that in frame 6.) The plots are histograms that have been normalised to represent a probability distribution (plotted on the vertical axis) and hence there is a small amount of statistical fluctuation due to the finite sample size of 10,000.

of resolving any conventional broadening the effects of nonequilibrium could dominate. For instance, the Fermi-LAT has a resolution of approximately 10% and a WIMP annihilation line is expected to have an intrinsic spread of only 0.1%. So if there were any quantum nonequilibrium present in the detected signal, we would expect the effects to have a lengthscale roughly two orders of magnitude larger than the expected line width. To further illustrate this point we note that, in figure 3, the broadenings in the $T = 5$ and $T = 1000$ frames may appear to be roughly equal. But in fact they are not as the energy dispersion is 20% in the former and only 0.1% in the latter so that the broadening is approximately 200 times larger in the former case. Thus while the broadening in the latter case may be confused with broadening from conventional sources, the former may very well dominate conventional effects. Note that to draw this conclusion on lengthscales we have not had to invoke any particular aspects of our model and so we expect this to be a general feature of nonequilibrium spectral lines.

The second category of characteristic modifications arises from the effects of dynamical relaxation. These effects are model dependent. In our model the precision of a reading is proportional to gt/σ_y. So although we have been considering the duration t of the measurement to determine its precision we could keep the duration fixed and consider the accuracy of a reading to be a function of σ_y (the uncertainty in the pointer position). The model indicates that readings of higher precision will disturb any initial nonequilibrium to a greater extent, allowing more opportunity for relaxation. Lower resolution telescopes would disturb nonequilibrium less and allow for less relaxation. So in addition to observing the effects on the largest scale, lower resolution telescopes may record the greatest deviations from equilibrium. In our simulations this regime corresponds to $T \lesssim 20$, or equivalently to an energy dispersion of $\Delta E/E_\gamma \gtrsim 5\%$. Lines may appear shifted or widened and may display large tails. It is also common (among the nonequilibrium distributions we consider) to find tall narrow lines which may exist alone, in pairs, or in small groups (see figure 5). These lines may be conspicuously narrower than could conventionally be resolved by the model telescope. For certain mid-resolution telescopes ($20 \gtrsim T \gtrsim 100$ or $5\% \gtrsim \Delta E/E_\gamma \gtrsim 1\%$ in our simulations), relaxation occurs but not to completion. In this case the fine structure in the configuration space distribution caused by partial relaxation may still be visible in the observed spectrum. Lines display small shelves or spikes in their profile, again on a lengthscale that could not conventionally

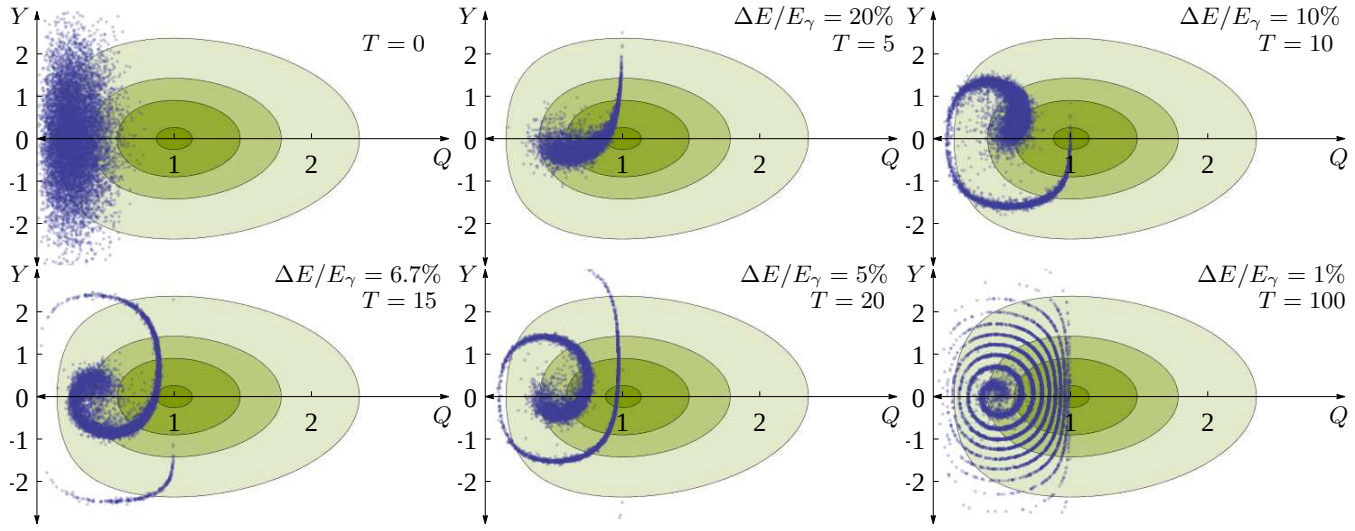

FIG. 4. The evolution of a nonequilibrium ensemble of spectral measurements (represented by 10,000 points). The initial nonequilibrium distribution for the field mode is equal to the equilibrium distribution narrowed by a factor of 4 (that is, $w = 1/4$). The individual trajectories that compose the nonequilibrium distribution are displayed in blue, while the equilibrium distribution is displayed in green. Only $Q > 0$ is shown as the behaviour is identical for $Q < 0$. Each frame displays the state at particular time T in the evolution, and equally (since $\Delta E/E_\gamma = T^{-1}$) each frame displays the results of measurements at the given resolution. Distributions that are narrower than quantum equilibrium will tend to have most of their support confined to the region $|Q| < 1$ (cf. figure 1). In this region of the configuration space the trajectories are roughly circular (unless they begin extremely close to $Q = \pm 1$ or $Q = 0$). As such, for a sufficiently high resolution model telescope, the partial relaxation that occurs yields a nonequilibrium spectral line which closely approximates equilibrium. For lower resolution telescopes, that do not disturb the nonequilibrium very much, these narrowed distributions tend to display narrowed single or multiple lines. This is the case for frames 2 to 5. The spectral line profiles that correspond to these frames are shown in figure 5.

be resolved. A final regime exists for telescopes of sufficient resolution that they disturb the nonequilibrium significantly. In these cases, we expect not to be able to resolve any of the fine structure that is the remnant of relaxation. For real telescopes of this resolution it may be that equilibrium is actually reached, but in our model the relaxation can be only partially achieved. (Indeed it is already known [13] that for sufficiently simple quantum systems de Broglie-Bohm trajectories need not explore the entire support of $|\psi|^2$, in which case nonequilibrium does not entirely decay.) Beyond a resolution of about $\Delta E/E_\gamma = 1\%$ our model produces a spectral line which is stationary on the lengthscale $\Delta E/E_\gamma$ and which is characteristic of the initial nonequilibrium present. In this regime, nonequilibrium distributions that are initially wider (in the field coordinate Q) than equilibrium produce wider lines whilst the initially narrower distributions produce lines often closely resembling $D(E|E_\gamma)$, although sometimes exhibiting a box-like profile.

Before moving to the next section, we shall briefly address the case in which the system had not been reduced to two dimensions as it was at the beginning of this section. Then, the configuration of a system is specified by $(Q, Y', \{Q_{\mathbf{k}sr}\})$ and this configuration is guided by

$$\partial_T Q = \frac{1}{6}\left(\frac{1}{Q} - Q\right) Y', \quad \partial_T Q_{\mathbf{k}sr} = -\frac{1}{6}\frac{E_\mathbf{k}}{E_\gamma} Q_{\mathbf{k}sr} Y',$$
$$\partial_T Y' = \frac{1}{6Q^2} + \frac{1}{3}Q^2 - \frac{5}{6} + \sum_{\mathbf{k}sr} \frac{E_\mathbf{k}}{E_\gamma}\left(\frac{1}{3}Q_{\mathbf{k}sr}^2 - \frac{1}{6}\right). \tag{37}$$

These feature a sum over all vacuum field modes, and as such are difficult to treat numerically. We may however attempt to employ the same strategy that allowed us to arrive at the paths (34). We may find a function G that is conserved along trajectories by solving $v.\nabla G = 0$, where v is a vector containing the guidance equations (37). For a particular choice of integration constants, this yields

$$G = \frac{1}{2}Y'^2 + Q^2 - \ln|Q| - \ln|Q^2 - 1| + \sum_{\mathbf{k}sr}\left(Q_{\mathbf{k}sr}^2 - \ln|Q_{\mathbf{k}sr}|\right). \tag{38}$$

in analogy with equation (34). The trajectories described by guidance equations will then traverse hypersurfaces of constant G. As with the paths (34), these surface are stationary with respect to the lengthscale $\Delta E/E_\gamma$. Consequently we expect the spectral features produced by this multi-mode case to exhibit the same characteristic lengthscale $(\Delta E/E_\gamma)$ as that seen in the reduced model

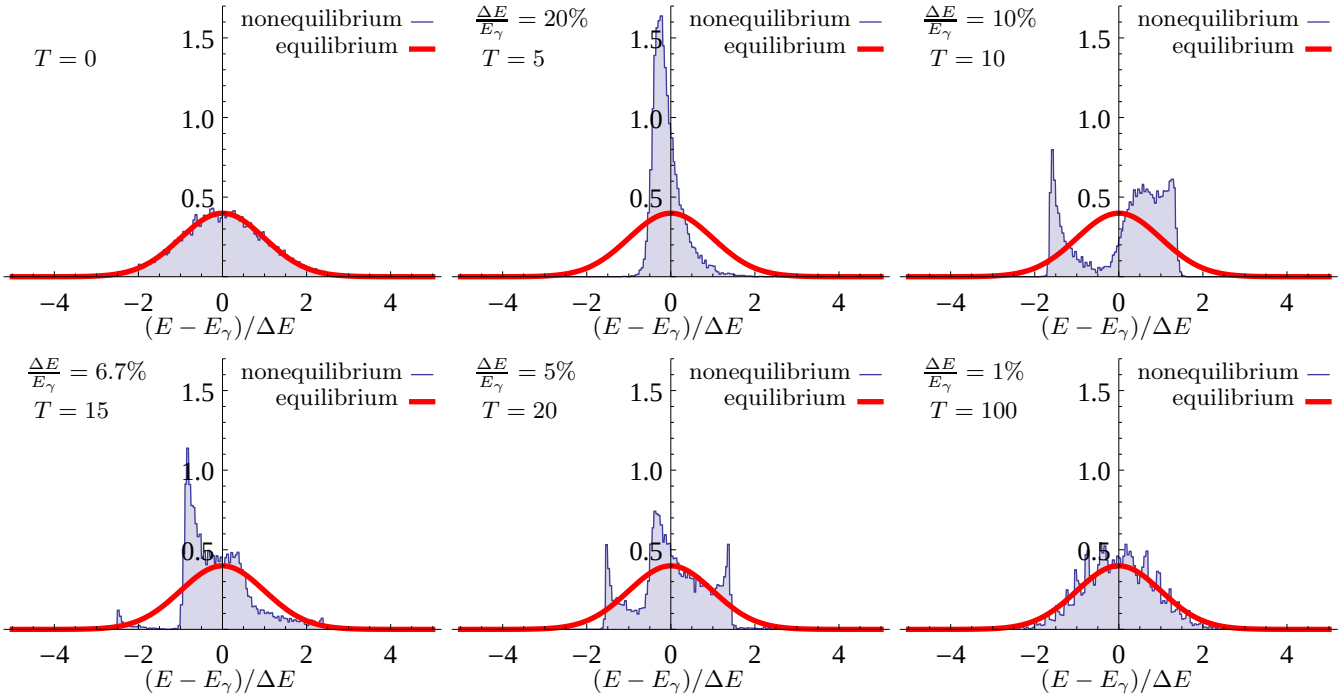

FIG. 5. Spectral line profiles produced by an initial $w = 1/4$ quantum nonequilibrium (corresponding to the frames shown in figure 4), contrasted with the equilibrium line (the standard energy dispersion function $D(E|E_\gamma)$). Each frame corresponds to a model telescope with different resolution. (For instance, the third frame shows a line produced by a model telescope with a roughly Fermi-LAT resolution of $\Delta E/E_\gamma = 10\%$.) The lines are given by the marginal distributions of the frames in figure 4. The energies that are recorded are measured in units of the energy dispersion of the frame. (For example, in absolute energy units and for a given value of E_γ, the equilibrium spectral line in frame 3 is 10 times the width of that in frame 6.) The plots are histograms that have been normalised to represent a probability distribution (plotted on the vertical axis) and hence there is a small amount of statistical fluctuation due to the finite sample size of 10,000. Frames 2 to 5 show examples of the transient behaviour that nonequilibrium can produce. Each of these frames exhibits spectral profiles that are narrower than a telescope should conventionally be able to resolve. Frame 3 shows the formation of a double bump–a common feature produced by initial nonequilibrium distributions that are narrower than equilibrium. Frame 6 shows the formation of the fine structure that is a hallmark of quantum relaxation.

that has been the focus of our discussion. The effect of the inclusion of the vacuum modes upon the transient features caused by relaxation is more unclear. It could be that the inclusion of the vacuum modes allows for efficient relaxation to equilibrium even during the measurement process itself. Although some preliminary numerical work indicates that the trajectories remain periodic when at least up to ten vacuum modes are included and we think it likely that periodic trajectories would limit the extent of the relaxation that takes place. It could be that any nonequilibrium statistics would be lost in the additional configuration space dimensions and not appear in the marginal pointer distribution. Although, since all field modes are coupled only indirectly to each other through the pointer, any transferral of nonequilibrium from any individual field mode to any another would necessarily transfer through the pointer statistics, which would act as a intermediary in the process. We might therefore expect the pointer to retain a large portion of any notion of a nonequilibrium 'budget' we could attempt to introduce. It is of course also very possible that spectral features would be produced that are similar to those that we have discussed for the reduced model. Further discussion on this point will left for future work.

IV. POSSIBLE IMPLICATIONS FOR THE INDIRECT SEARCH FOR DARK MATTER

We now discuss of the limitations of our arguments and the possible implications for the indirect search for dark matter. The inner workings of contemporary gamma-ray telescopes are complicated, typically involving a great many interactions before an estimate of the incident photon energy may be made. The extent to which our idealised von Neumann type spectral measurement will reflect the properties of such telescopes is therefore open to question. Indeed, the complexities of a real telescope might even degrade any incoming nonequilibrium making it effectively unobservable. To discount this possibility would require a much more complicated (and potentially intractable) model. A description of quantum nonequilibrium requires a solution to the (functional) Schrödinger equation and this may never be practical in such a context (at least in the foreseeable future). Our simple model can only hope to capture some of the es-

sential physics and to illustrate the kinds of effects that might be generated by incoming nonequilibrium photons. Our model may be oversimplified, but it does yield distinctive physical effects which could be searched for in the data and which would be difficult to account for in terms of standard physics. If such effects were observed, one would have to weigh the possible discovery of quantum nonequilibrium against possible rival explanations. It would be for other model builders to construct rival interpretations of the effects predicted here (should they be observed).

We have argued that the consequence of quantum nonequilibrium is to effect the change $D(E|E_\gamma) \rightarrow D_{\text{noneq}}(E|E_\gamma)$ and that this change must take place on lengthscales of order $\Delta E/E_\gamma$. This lengthscale measures the resolution of the telescope, which in many circumstances may be orders of magnitude larger than conventional line broadening. We have seen this assertion reflected in the behaviour of our model.

In our model the spread of the standard (equilibrium) line spectrum $D(E|E_\gamma)$ is attributable to the initial uncertainty in the pointer, a quantum uncertainty. For a real telescope, however, the spread in $D(E|E_\gamma)$ will be only partly quantum in nature and partly of classical origin. In a circumstance in which the spread is predominately classical, we would expect the nonequilibrium signatures to be suppressed. To study this further would require a more realistic model of a specific telescope.

With this in mind, and in the absence of any nonequilibrium distributions that are more extreme than those we have considered, it seems highly likely that the confirmed discovery of a DM spectral line would need to precede any investigation into the cause of an anomalous line shape. After all, signal statistics that are significant enough to prove that a spectral line has an anomalous shape would surely be significant enough to prove the existence of the line in the first place. Even so the presence of nonequilibrium could be relevant to the indirect search for dark matter. In particular, the presence of quantum nonequilibrium in the signal photons could obfuscate the detection process and make the discovery of a spectral line more elusive. For example, substantial nonequilibrium broadening could make the line difficult to distinguish from the background (cf. figure 3). Furthermore, nonequilibrium narrowing could lead to severe misinterpretations of the data.

This last point may be illustrated by the case of the controversial ∼130GeV line-like feature reported in the Fermi-LAT data in 2012 [41, 42]. One of the original reasons why this feature was discredited as an actual signal was that it seemed too narrow. In 2013 the Fermi collaboration disputed the existence of the line, arguing that 'the feature is narrower than the LAT energy resolution at the level of 2 to 3 standard deviations, which somewhat disfavours the interpretation of the 133 GeV feature as a real WIMP signal' [43]. As we have seen, features narrower than the expected energy resolution can occur as a result of quantum nonequilibrium. We have also seen that narrow nonequilibrium can generate multiple lines (cf. figure 5). Remarkably, the authors of refs. [44] and [45] found that the feature was marginally better fit by two lines at ∼111GeV and ∼129GeV. The energy resolution of the LAT is approximately $\Delta E/E_\gamma \approx 10\%$ in this energy range and it so happens that in our model narrowed incoming nonequilibrium tends to display narrowed spectral profiles and double lines for model telescopes with a resolution of ∼10% (see the third frame of figure 5.) Of course, we certainly do not wish to give the impression that we attribute the ∼130GeV feature to a nonequilibrium signal. The current consensus appears to be that the apparent feature was caused by an unfortunate combination of a small sample size and systematic error, with more recent studies having access to more data reporting a reduced significance [46, 47]. However, it is worth drawing attention to the parallels between recent claims about this particular feature and the effects that naturally emerge from our model–if only to illustrate how the presence of a narrowed nonequilibrium in the incident photons could cause difficulties with the interpretation of the data.

As we have noted, we would expect the discovery of a line to be confirmed before any significant inquiry into the cause of an anomalous profile. If however such a line were unequivocally detected and its anomalous profile was distinct and persisted, there would be calls for other telescopes to replicate the profile. From our point of view this could prove problematic as, even in our idealised model, two telescopes of differing resolution would observe differing profiles. Furthermore, for real telescopes, even two of identical resolution may work by differing mechanisms and react to the nonequilibrium differently. It is possible that a hypothesis of nonequilibrium would be supported by its characteristic lengthscale. On the other hand the complex workings of a second telescope might cause complete relaxation during its measurement process, resulting in a line profile consistent with equilibrium. In this case it would be tempting to conclude that the second telescope was the 'more correct' thereby further confounding the matter. On this point it would be helpful to design an experiment with only minimal opportunity for relaxation. Perhaps the matter could be resolved by performing independent tests searching for nonequilibrium signatures in incoming photons that are suspected of carrying nonequilibrium–for example, deviations from Malus' law in their polarisation probabilities [48].

In de Broglie-Bohm theory, individual members of an ensemble have definite configurations and together may be thought of as defining the ensemble probability distribution to which they belong. One may therefore consider combining two differing nonequilibrium ensembles to create a third distinct nonequilibrium ensemble. In an empirical context one will necessarily take a pragmatic approach to how the relevant ensemble is to be defined. For example one might consider systems in a particular region of the sky, or in a set of regions surrounding a par-

ticular type of astrophysical object. There is no a priori reason why systems in different regions should exhibit the same nonequilibrium statistics. This again may be a potential barrier reproducibility of results. On the other hand, if an ensemble of similar astrophysical objects produced similar spectra except in a region where a dark matter spectral line is suspected or known to exist, then a hypothesis of nonequilibrium might be supported.

There are clearly many ways in which our effects could manifest in the search for dark matter, and there are many practical reasons why our effects could turn out to be obscured even if they exist. More work remains to be done on these matters. Only time will tell whether any of the scenarios we have outlined will prove to be informative.

[1] L. de Broglie, in *Électrons et Photons: Rapports et Discussions du Cinquième Conseil de Physique* (Gauthier-Villars, Paris, 1928) [English translation in ref. [2]].

[2] G. Bacciagaluppi and A. Valentini, *Quantum Theory at the Crossroads: Reconsidering the 1927 Solvay Conference* (Cambridge University Press, Cambridge, 2009) arXiv:quant-ph/0609184 [quant-ph].

[3] D. Bohm, A suggested interpretation of the quantum theory in terms of "hidden" variables. I, Phys. Rev. **85**, 166 (1952).

[4] D. Bohm, A suggested interpretation of the quantum theory in terms of "hidden" variables. II, Phys. Rev. **85**, 180 (1952).

[5] P. R. Holland, *The Quantum Theory of Motion: an Account of the de Broglie-Bohm Causal Interpretation of Quantum Mechanics* (Cambridge University Press, Cambridge, 1993).

[6] A. Valentini, Signal-locality, uncertainty, and the subquantum H-theorem. I, Phys. Lett. A **156**, 5 (1991).

[7] A. Valentini, *On the Pilot-Wave Theory of Classical, Quantum and Subquantum Physics*, Ph.D. thesis, International School for Advanced Studies, Trieste, Italy (1992).

[8] A. Valentini, in *Chance in Physics: Foundations and Perspectives*, edited by J. Bricmont *et al.* (Springer, Berlin, 2001) arXiv:quant-ph/0104067.

[9] A. Valentini and H. Westman, Dynamical origin of quantum probabilities, Proc. R. Soc. A **461**, 253 (2005), arXiv:quant-ph/0403034 [quant-ph].

[10] S. Colin, Relaxation to quantum equilibrium for Dirac fermions in the de Broglie-Bohm pilot-wave theory, Proc. R. Soc. A **468**, 1116 (2012), arXiv:1108.5496 [quant-ph].

[11] C. Efthymiopoulos and G. Contopoulos, Chaos in Bohmian quantum mechanics, J. Phys. A: Math. Gen. **39**, 1819 (2006).

[12] M. D. Towler, N. J. Russell, and A. Valentini, Time scales for dynamical relaxation to the Born rule, Proc. R. Soc. A **468**, 990 (2012), arXiv:1103.1589 [quant-ph].

[13] E. Abraham, S. Colin, and A. Valentini, Long-time relaxation in pilot-wave theory, J. Phys. A: Math. Theor. **47**, 395306 (2014), arXiv:1310.1899 [quant-ph].

[14] A. Valentini, Signal-locality, uncertainty, and the subquantum H-theorem. II, Phys. Lett. A **158**, 1 (1991).

[15] A. Valentini, in *Bohmian Mechanics and Quantum Theory: An Appraisal*, edited by J. T. Cushing, A. Fine, and S. Goldstein (Kluwer, Dordrecht, 1996).

[16] A. Valentini, Subquantum information and computation, Pramana J. Phys. **59**, 269 (2002), arXiv:quant-ph/0203049.

[17] A. Valentini, Astrophysical and cosmological tests of quantum theory, J. Phys. A: Math. Theor. **40**, 3285 (2007), arXiv:hep-th/0610032 [hep-th].

[18] A. Valentini, De Broglie-Bohm prediction of quantum violations for cosmological super-Hubble modes, (2008), arXiv:0804.4656 [hep-th].

[19] A. Valentini, Beyond the quantum, Phys. World **22N11**, 32 (2009), arXiv:1001.2758 [quant-ph].

[20] A. Valentini, Inflationary cosmology as a probe of primordial quantum mechanics, Phys. Rev. D **82**, 063513 (2010), arXiv:0805.0163 [hep-th].

[21] A. Valentini, in *Many Worlds? Everett, Quantum Theory, & Reality*, edited by S. Saunders *et al.* (Oxford University Press, Oxford, 2010) arXiv:0811.0810 [quant-ph].

[22] P. Pearle and A. Valentini, in *Encyclopaedia of Mathematical Physics*, edited by J.-P. Françoise *et al.* (Elsevier, North-Holland, 2006) arXiv:quant-ph/0506115 [quant-ph].

[23] S. Colin and A. Valentini, Mechanism for the suppression of quantum noise at large scales on expanding space, Phys. Rev. D **88**, 103515 (2013), arXiv:1306.1579 [hep-th].

[24] S. Colin and A. Valentini, Primordial quantum nonequilibrium and large-scale cosmic anomalies, Phys. Rev. **D92**, 043520 (2015), arXiv:1407.8262 [astro-ph.CO].

[25] N. G. Underwood and A. Valentini, Quantum field theory of relic nonequilibrium systems, Phys. Rev. **D92**, 063531 (2015), arXiv:1409.6817 [hep-th].

[26] W. B. Atwood *et al.*, The Large Area Telescope on the Fermi Gamma-Ray Space Telescope mission, Astrophys. J. **697**, 1071 (2009).

[27] D. J. Thompson *et al.*, Calibration of the Energetic Gamma-Ray Experiment Telescope (EGRET) for the Compton Gamma-Ray Observatory, Astrophys. J. Suppl. Ser. **86**, 629 (1993).

[28] C. Jin, Dark Matter Particle Explorer: The first Chinese cosmic ray and hard γ-ray detector in space, Chin. J. Space Sci. **34**, 550 (2014).

[29] N. P. Topchiev *et al.*, The GAMMA-400 experiment: Status and prospects, Bull. Rus. Acad. Sci: Phys. **79**, 417 (2015).

[30] L. Bergström and H. Snellman, Observable monochromatic photons from cosmic photino annihilation, Phys. Rev. D **37**, 3737 (1988).

[31] S. Rudaz, On the annihilation of heavy neutral fermion pairs into monochromatic gamma-rays and its astrophysical implications, Phys. Rev. **D39**, 3549 (1989).

[32] L. Bergström and P. Ullio, Full one-loop calculation of neutralino annihilation into two photons, Nucl. Phys. **504**, 27 (1997).

[33] L. Bergström, T. Bringmann, M. Eriksson, and M. Gustafsson, Two photon annihilation of Kaluza-Klein dark matter, J. Cosmol. Astropart. Phys. **0504**, 004 (2005), arXiv:hep-ph/0412001 [hep-ph].

[34] G. Bertone, C. B. Jackson, G. Shaughnessy, T. M. P. Tait, and A. Vallinotto, Gamma ray lines from a universal extra dimension, J. Cosmol. Astropart. Phys. **1203**, 020 (2012), arXiv:1009.5107 [astro-ph.HE].

[35] L. Bergström, Dark matter evidence, particle physics candidates and detection methods, Annalen Phys. **524**, 479 (2012), arXiv:1205.4882 [astro-ph.HE].

[36] M. Ackermann *et al.*, The Fermi Large Area Telescope on orbit: Event classification, instrument response functions, and calibration, Astrophys. J. Suppl. Ser. **203**, 4 (2012).

[37] S. N. Zhang *et al.*, The High Energy Cosmic-Radiation Detection (HERD) facility onboard china's space station, Proc. SPIE **9144**, 91440X (2014).

[38] W. Johnson, J. Grove, B. Phlips, J. Norris, and A. Moiseev, A CsI(Tl) hodoscopic calorimeter for the glast mission, *Nuclear Science Symposium, 1997. IEEE*, , 27 (1997).

[39] L. I. Schiff, *Quantum Mechanics* (McGraw-Hill, 1968).

[40] W. Struyve and A. Valentini, De Broglie-Bohm guidance equations for arbitrary Hamiltonians, J. Phys. A: Math. Theor. **42**, 035301 (2009), arXiv:0808.0290 [quant-ph].

[41] T. Bringmann, X. Huang, A. Ibarra, S. Vogl, and C. Weniger, Fermi LAT search for internal bremsstrahlung signatures from dark matter annihilation, J. Cosmol. Astropart. Phys. **1207**, 054 (2012), arXiv:1203.1312 [hep-ph].

[42] C. Weniger, A tentative gamma-ray line from dark matter annihilation at the fermi large area telescope, J. Cosmol. Astropart. Phys. **1208**, 007 (2012), arXiv:1204.2797 [hep-ph].

[43] M. Ackermann *et al.* (Fermi-LAT Collaboration), Search for gamma-ray spectral lines with the fermi large area telescope and dark matter implications, Phys. Rev. D **88**, 082002 (2013), arXiv:1305.5597 [astro-ph.HE].

[44] M. Su and D. P. Finkbeiner, Strong evidence for gamma-ray line emission from the inner galaxy, (2012), arXiv:1206.1616 [astro-ph.HE].

[45] M. Su and D. P. Finkbeiner, Double gamma-ray lines from unassociated Fermi-LAT sources, (2012), arXiv:1207.7060 [astro-ph.HE].

[46] B. Anderson, S. Zimmer, J. Conrad, M. Gustafsson, M. Sánchez-Conde, and R. Caputo, Search for gamma-ray lines towards galaxy clusters with the Fermi-LAT, J. Cosmol. Astropart. Phys. **1602**, 026 (2016), arXiv:1511.00014 [astro-ph.HE].

[47] M. Ackermann *et al.* (Fermi-LAT), Updated search for spectral lines from galactic dark matter interactions with pass 8 data from the Fermi Large Area Telescope, Phys. Rev. **D91**, 122002 (2015), arXiv:1506.00013 [astro-ph.HE].

[48] A. Valentini, Universal signature of non-quantum systems, Phys. Lett. A **332**, 187 (2004), arXiv:quant-ph/0309107.